

GaAs/AlGaAs- and InGaAs/AlGaAs-heterostructures for high-power semiconductor infrared emitters

© D.V. Gulyaev,¹ D.V. Dmitriev,¹ N.V. Fateev,¹ D.Yu. Protasov,^{1,2} A.S. Kozhukhov,¹ K.S. Zhuravlev¹

¹Rzhanov Institute of Semiconductor Physics,
630090 Novosibirsk, Russia

²Siberian Branch, Russian Academy of Sciences,
630073 Novosibirsk, Russia
e-mail: gulyaev@isp.nsc.ru

Received May 12, 2021

Revised June 28, 2021

Accepted July 1, 2021

The internal quantum efficiency of GaAs/AlGaAs- and InGaAs/AlGaAs-heterostructures for infrared light emitter diodes has been determined. The influence of the growth conditions of heterostructures grown by the molecular beam epitaxy and post-growth annealing on the quantum efficiency of heterostructures has been investigated. It has been shown that it is possible to increase the quantum luminescence efficiency of the studied heterostructures up to 75–80% at the average power by the combined optimization of these processes.

Keywords: GaAs/AlGaAs and InGaAs/AlGaAs heterostructures, internal quantum exit, photoluminescence, molecular-beam epitaxy.

DOI: 10.21883/TP.2022.14.55226.142-21

Introduction

IR light-emitting devices are interesting for their invisibility to the human eye, with the possibility of detecting radiation by electronic systems from photodetectors to conventional video cameras. That is why infrared light emitted diodes with a wavelength of 850 to 980 nm are most widely used as part of IR sensors, indispensable in almost all areas of our life: from domestic appliances (control panels, security systems) and medical equipment (pulse oximeters) to process control (item counter and position sensors, automation) [1–3].

The main characteristic of such emitting devices, by definition, is luminosity. Increase in the luminosity of emitting devices without changing their design is possible as a result of increasing in the internal and external quantum efficiency. To increase the external quantum efficiency, the most common methodology are used, such as the formation of a reflective surface under the active region of the device [4–6], photonic crystals [7,8], increasing the surface roughness [9,10] and/or applying antireflection coatings [14]. However, without a good basis, namely the heterostructure with high internal quantum yield, the application of these methodologies will not provide the high performance light emitting diode. Increase in the internal quantum yield is primarily achieved by selecting optimal conditions for the growth of [12] heterostructure, which ensures high crystalline perfection of the structure and the absence of nonradiative recombination centers. Depending on the conditions and methods of manufacturing molecular-beam epitaxy (MBE) [13,14] or metalorganic vapour phase epitaxy [15,16]), the internal quantum yield of structures can vary within fairly wide limits, reaching in the best

samples over 90% [13–18]. In the works, however, the power at which the measurement was carried out is by no means always indicated, which often makes it impossible to compare literature data with each other, since the quantum yield depends on the pumping power.

In this work, we present the results of MBE preparing of GaAs/AlGaAs and InGaAs/AlGaAs quantum-well (QW) heterostructures, which are intended for fabrication of LEDs based on them for operation in the near-IR range.

1. Experimental procedure

The studied heterostructures with GaAs/AlGaAs or InGaAs/AlGaAs quantum wells were grown by MBE on the GaAs substrate heavily doped with (100) orientation, with GaAs buffer layer 0.4 μm thick. The construction of the grown heterostructures (see Table) corresponds to the construction of heterostructures for high-power semiconductor infrared emitters with one exception: there is no upper 3–6 μm AlGaAs spreading layer, since the upper contact layer (band gap 1.67 eV) in its presence absorbs all the radiation of the laser that excites luminescence (2.35 eV) and makes it impossible to determine the internal quantum yield of the heterostructure using the photoluminescence (PL) method used in the work. For each type of QW (GaAs/AlGaAs or InGaAs/AlGaAs), a series of samples were grown at different growth temperatures: the growth temperatures of GaAs/AlGaAs QWs varied from 590 to 620 °C, and of InGaAs/AlGaAs QWs from 480 to 525 °C respectively. The growth temperatures were determined from the reconstruction transitions on the growth surface in the fast electron diffraction during reflection. The

Construction of GaAs/AlGaAs and InGaAs/AlGaAs heterostructures

№	Purpose	Material	Thickness, nm	Composition (x at $\text{Me}_x\text{Ga}_{1-x}\text{As}$)	Doping, cm^{-3}
6	Upper contact	GaAs	30		$\text{C}: 5 \cdot 10^{18}$
5	Upper blocking layer	AlGaAs	60	0.2	$\text{C}: 5 \cdot 10^{18}$
4	Active region (7 periods QW)	AlGaAs	16	0.2	
		GaAs/InGaAs (for $\lambda = 860/905$ nm)	15/12 (for $\lambda = 860/905$ nm)	-/0.075	
3	Lower blocking layer		60	0.2	$\text{Si}: 3 \cdot 10^{18}$
2	Mirror on the basis distributed Bragg reflector (3 periods)	AlGaAs	62/65 (for $\lambda = 860/905$ nm)	0.1	$\text{Si}: 3 \cdot 10^{18}$
		AlGaAs	71/74 (for $\lambda = 860/905$ nm)	0.9	$\text{Si}: 3 \cdot 10^{18}$
1	Buffer layer	GaAs	500		$\text{Si}: 3 \cdot 10^{18}$
0	Substrate	GaAs	400000		$\text{Si}: 3 \cdot 10^{18}$

additionally grown heterostructures were annealed at various temperatures from 700 to 850°C in neutral nitrogen atmosphere for 3 min. To prevent the desorption of atoms during annealing, a layer of SiO_2 about 100 nm thick was preliminarily deposited on the surface of the samples. To characterize the samples, the surface of their cleavage was studied by atomic force microscopy (AFM) in modes that provided the best image contrast, namely, Kelvin's scanning probe microscopy and registration of adhesion forces [19]. Appearance of the additional adhesion force between the surface and the probe when it is uncoupled is a consequence of the presence of a water meniscus on the surface of the measured sample. The magnitude of adhesion in this case depends on the structure and material of the surface, which makes it possible to study its features with good lateral resolution even in the absence of significant surface gradients in its height.

The internal quantum yield of the heterostructures was determined from the analysis of the PL data. The PL was excited by YAG:Nd laser with wavelength of 527 nm and maximum power of 150 mW/mm². The diameter of the laser spot on the sample was 1 mm². As a reference sample, a solution of rhodamine 6G in ethanol was used, which at wavelength of 527 nm has the quantum yield close to 100% [20,21]. PL was recorded with the spectrometer based on single monochromator equipped with a silicon CCD (charge-coupled device) camera. Measurements were performed at room temperature.

2. Experimental results and discussion

The AFM image of the sample cleavage near the active region is shown in Fig. 1. Quantum wells are clearly visible

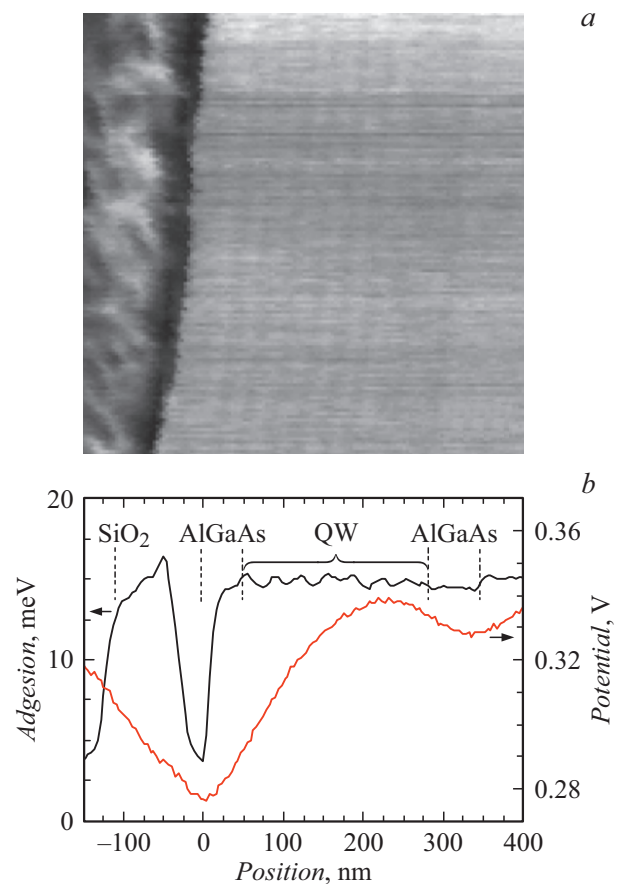


Figure 1. *a* — AFM image ($0.55 \times 0.55 \mu\text{m}$); *b* — adhesive force profile and surface potential distribution near the active region of the sample.

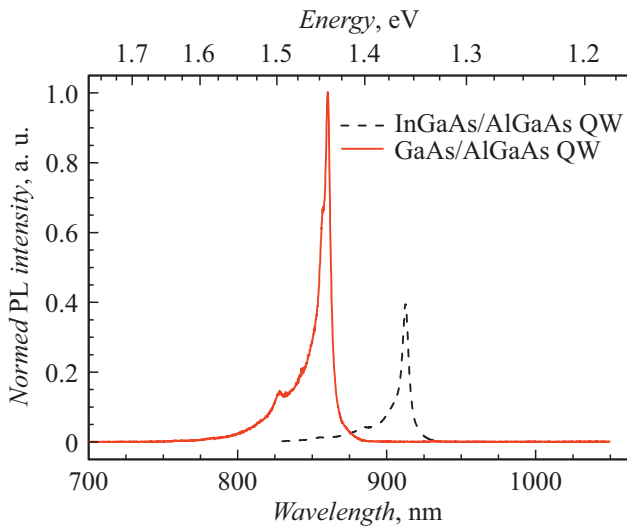


Figure 2. Typical PL spectra of GaAs/AlGaAs and InGaAs/AlGaAs QWs at room temperature. Laser excitation power is 20 mW.

on the AFM image in the mode of adhesion of forces, and the upper and lower blocking AlGaAs layers correspond to the minima of the potential measured by Kelvin probe microscopy and expressing the work function for escaping from material.

Figure 2 shows the PL spectra of test GaAs/AlGaAs and InGaAs/AlGaAs heterostructures for 860 and 905 nm, respectively. The PL spectra of both sample types are dominated by the band associated with recombination between size quantization levels in QWs with full width at half maximum (FWHM) of about 10 meV at 300 K.

The internal quantum yield was determined from the luminescence data using the standard ABC model, which takes into account radiative recombination, nonradiative Shockley-Read recombination, and Auger recombination. To simplify the calculation of the internal quantum yield, the experimental dependence of the stationary PL intensity of the samples on the laser excitation power (Fig. 3,a) was transformed into the inverse function $P_{laser}(I_{PL}) = P_1 I_{PL}^{0.5} + P_2 I_{PL} + P_3 I_{PL}^{1.5}$. That sort of approach makes it possible to determine the internal quantum yield at arbitrary excitation power without knowing the coefficients A, B and C in the continuity equations [22]. In this case, the internal quantum yield of structures is determined from the formula $\eta = P_2 I_{PL} / P_{laser}$, where P_2 is adjustable parameter depending on $P_{laser}(I_{PL})$, independent of the rate of radiative and nonradiative recombination in the material under study. Indeed, according to [22], $P_2 = 1/(xa)$, where a is the constant determined by the volume of the excited region and the luminescence collection efficiency, and $x = (1 - R)\alpha / (A_{SPOT} h\nu)$, where R is reflection from the sample surface, α is absorption coefficient, A_{SPOT} is area of the laser beam on the sample, $h\nu$ is photon energy.

Additionally, the quantum yield of the samples was estimated from comparison of the PL intensities of the

samples with the PL of rhodamine 6G, which has the quantum yield of 96% [20] at a wavelength of 527 nm. The obtained data coincided with the data obtained from the analysis of the power dependence of the PL with accuracy of several percent. The results of calculating the quantum yield for unannealed heteroepitaxial structure (HES) samples are shown in Fig. 3, b. As can be seen, the internal quantum yield of GaAs/AlGaAs structures is much higher than that of InGaAs/AlGaAs structures. This difference is the consequence of growing In-containing QWs at temperatures lower by 100°C compared to structures with GaAs QWs, which leads to the increase in the concentration of nonradiative recombination centers [23].

Since the quantum yield of the samples depends on the laser excitation power (Fig. 3, b), the average power of 20 mW was chosen to compare the samples with each other. The dependences of the quantum yield of heterostructures with InGaAs/AlGaAs and GaAs/AlGaAs QWs on the growth temperature for this power are shown in Fig. 4, a. It can be seen that for both types of HES, the optimal growth temperature, the deviation from which causes the decrease in the internal quantum yield, is present. This behavior is

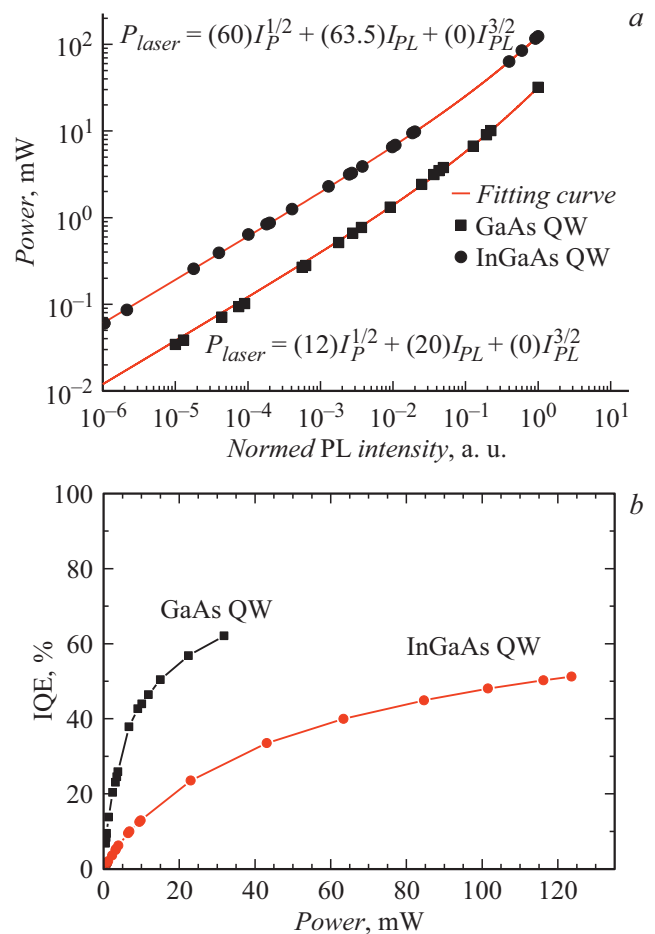


Figure 3. Dependences of the (a) PL intensity and (b) quantum yield on the laser excitation power for unannealed GaAs and InGaAs QWs. The growth temperatures of GaAs/AlGaAs and InGaAs/AlGaAs QWs are 510 and 610°C, respectively.

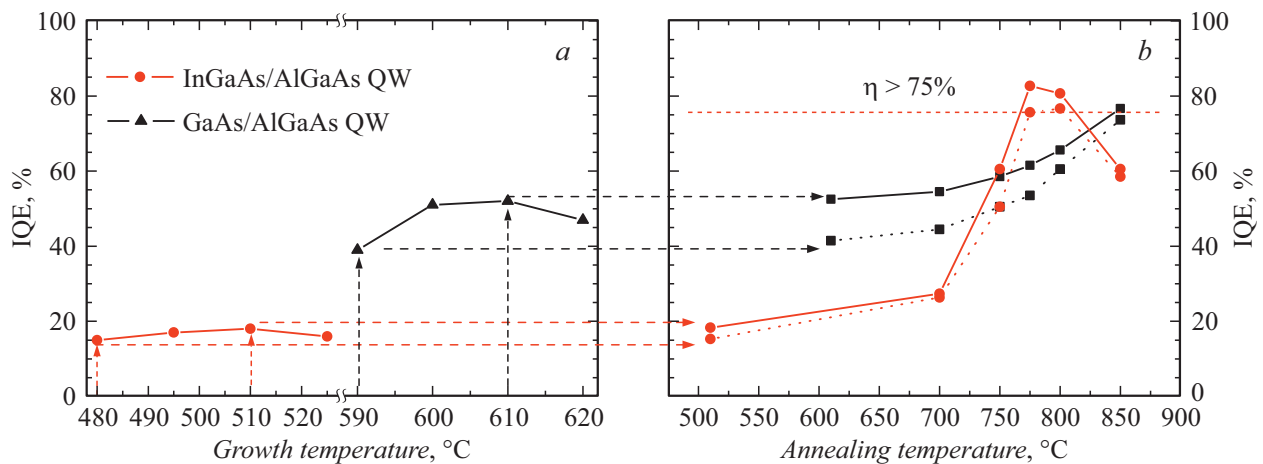


Figure 4. Dependence of the internal quantum yield of the luminescence of heterostructures with InGaAs/AlGaAs and GaAs/AlGaAs QWs on the growth temperature (a) and the annealing temperature (b). Laser excitation power is 20 mW.

explained by the competition of two processes depending on the growth temperature:

- 1) because of the increases in the migration of poorly integrated adatoms of the 3 group (Ga, Al) over the surface, which reduces the number of growth defects;
- 2) because of the segregation and desorption of Ga and/or In atoms with increasing temperature, which, on the contrary, increases the concentration of defects [24,25].

Compensation for the desorption of Ga and/or In atoms during MBE with increasing temperature is possible by increasing the ratio of the atom flows of the 3 and 5 groups, however, this leads to a strong overconsumption of materials of the 3 group and is not applicable for typical MBE-technology for preparation of heterostructures, which is the compromise between the consumption of materials and the quality of the structure.

It is known from the literature that the concentration of defects in A3B5 materials obtained by MBE can be reduced by temperature annealing [26–28]. Figure 4, b shows the results of short-term annealing of samples grown at optimal growth temperatures. It can be seen that the increase in the quantum yield of the InGaAs QW occurs only up to the temperature of 775°C, while the quantum yield of the GaAs QW increases to the temperature of 850°C. Such a difference between In-containing QWs can be explained by their „intermixing“ due to the onset of diffusion of indium atoms between the barrier and the well at these temperatures [29,30]. This statement is confirmed by the shift of the energy position of the lines at 1 meV observed in the PL spectra of InGaAs/AlGaAs QWs annealed at 850°C. The maximum quantum yield of In-containing structures, despite the lower annealing temperature, turns out to be somewhat higher than that of the GaAs QW, which is caused by the large value of the matrix element of the optical transition in the InGaAs QW due to its smaller thickness (12 nm instead of 15 nm for GaAs QW). In any case, it can be seen that the quantum yield of both GaAs/AlGaAs HESs and InGaAs/AlGaAs structures can be

increased by short-term annealing in neutral atmosphere to values of 75–80%. Wherein, it should be noted that this result was achieved using arsenic with a purity of only 99.99995% (6N), and it can be expected that the use of purer starting materials of the 7N type will further increase the internal luminescence quantum yield of the heterostructure.

Conclusion

Thus, in the work, the study of internal luminescence quantum yield of GaAs/AlGaAs- and InGaAs/AlGaAs-heterostructures designed to create LEDs based on them for operation in the near-IR range, was carried out. The quantum yield is defined:

- 1) from the dependence of the PL intensity on the laser pumping power in the framework of the standard ABC model;
- 2) from the comparison of the PL intensities of the sample and standard.

It has been demonstrated that, by selecting the growth conditions for MBE-grown heterostructures, in combination with subsequent short-term annealing, it is possible to achieve the luminescence quantum yield of both GaAs/AlGaAs HES and InGaAs/AlGaAs structures of 75–80% at a moderate pumping power.

2.1. Acknowledgments

AFM measurements were carried out on the equipment of the CCU of Nanostructures of the Institute for Physical Problems, SB of the RAS.

Funding

The study was financially supported by the RFBR and the Novosibirsk Region under the scientific project № 20-42-540009.

Conflict of interest

The authors declare that they have no conflict of interest.

References

- [1] W.A. Cahyadi, Y. Ho Chung. *Opt. Express*, **26** (15), 19657 (2018). DOI: 10.1364/OE.26.019657
- [2] T. Tamura, Y. Maeda, M. Sekine, M. Yoshida. *Electronics*, **3**, 282 (2014). DOI: 10.3390/electronics3020282
- [3] A.C. Caputo. *Digital Video Surveillance and Security* (Elsevier Inc., 2014)
- [4] E.F. Schubert. *Light-emitting diodes (second edition)* (Cambridge University Press, 2006)
- [5] A.V. Malevskaya, N.A. Kalyuzhny, D.A. Malevsky, S.A. Mintairov, R.A. Saliy, A.N. Panchak, P.V. Pokrovsky, N.S. Potapovich, V.M. Andreev. *FTP*, **55** (7), 614 (2021) (in Russian) DOI: 10.21883/FTP.2021.07.51028.9646
- [6] S.-Y. Lee, E. Lee, J.-H. Moon, B. Choi, J.-T. Oh, H.-H. Jeong, T.-Y. Seong, H. Amano. *Photon. Technol. Lett. IEEE*, **32** (17), 1041 (2020). DOI: 10.1109/LPT.2020.3010820
- [7] H.-P.D. Yang, J.-N. Liu, F.-I. Lai, H.-Ch. Kuo, J.Y. Chi. *J. Modern Opt.*, **55** (9), 1509 (2008). DOI: 10.1080/09500340701691608
- [8] M. Li, H. Zhen, Y. Jing, H. Wang, N. Li. *Opt. Quant. Electron.*, **48** (2), 140 (2016). DOI: 10.1007/s11082-016-0415-3
- [9] I. Schnitzer, E. Yablonovitch, C. Caneau, T.J. Gmitter, A. Scherer. *Appl. Phys. Lett.*, **63** (16), 2174 (1993). DOI: 10.1063/1.110575
- [10] R. Windisch, C. Rooman, B. Dutta, A. Knobloch, G. Borghs, G.H. Dohler, P. Heremans. *IEEE J. Selected Topics in Quant. Electronics*, **8** (2), 248 (2002). DOI: 10.1109/2944.999177
- [14] T. Kato, H. Susawa, M. Hirotani, T. Saka, Y. Ohashi, E. Shichi, S. Shibata. *J. Crystal Growth*, **107** (1–4), 832 (1991). DOI: 10.1016/0022-0248(91)90565-M
- [12] S.-Ch. Ahn, B.-T. Lee, W.-Ch. An, D.-K. Kim, I.-K. Jang, J.-S. So, H.-J. Lee. *J. Korean Phys. Society*, **69** (1), 91 (2016). DOI: 10.3938/jkps.69.91
- [13] D. Ban, H. Luo, H.C. Liu, Z.R. Wasilewski, A.J. SpringThorpe, R. Glew, M. Buchanan. *J. Appl. Phys.*, **96** (9), 5243 (2004). DOI: 10.1063/1.1785867
- [14] R. Windisch, B. Dutta, M. Kuijk, A. Knobloch, S. Meinschmidt, S. Schoberth, P. Kiesel, G. Borghs, G.H. Dohler, P. Heremans. *IEEE Trans. Electron. Dev.*, **47** (7), 1492 (2000). DOI: 10.1109/16.848298
- [15] L. Han, M. Zhao, X. Tang, W. Huo, Z. Deng, Y. Jiang, W. Wang, H. Chen, Ch. Du, H. Jia. *J. Appl. Phys.*, **127** (8), 085706 (2020). DOI: 10.1063/1.5136300
- [16] I. Schnitzer, E. Yablonovitch, C. Caneau, T.J. Gmitter. *Appl. Phys. Lett.*, **62** (2), 131 (1993). DOI: 10.1063/1.109348
- [17] P. Bai, Y. Zhang, T. Wang, Z. Shi, X. Bai, Ch. Zhou, Y. Xie, L. Du, M. Pu, Z. Fu, J. Cao, X. Guo, W. Shen. *Semicond. Sci. Technol.*, **35** (3), 035021 (2020). DOI: 10.1088/1361-6641/ab6dbf
- [18] M.A. Ladugin, A.A. Marmalyuk, A.A. Padalitsa, K.Yu. Tegin, A.V. Lobintsov, S.M. Sapozhnikov, A.I. Danilov, A.V. Podkopaev, V.A. Simakov. *Quant. Electron.*, **47** (8), 693 (2017). DOI: 10.1070/QEL16441
- [19] A.L. Weisenhorn, P. Maivald, H.-J. Butt, P.K. Hansma. *Phys. Rev. B*, **45** (19), 11226 (1992). DOI: 10.1103/physrevb.45.11226
- [20] R.F. Kubin, A.N. Fletcher. *J. Luminescence*, **27** (4), 455 (1982). DOI: 10.1016/0022-2313(82)90045-X
- [21] P.A. Bokhan, N.V. Fateev, T.V. Malin, I.V. Osinnykh, D.E. Zakrevsky, K.S. Zhuravlev. *J. Luminescence*, **203** (4), 127 (2018). DOI: 10.1016/j.jlumin.2018.06.034
- [22] Y.-S. Yoo, T.-M. Roh, J.-H. Na, S.J. Son, Y.-H. Cho. *Appl. Phys. Lett.*, **102** (21), 211107 (2013). DOI: 10.1063/1.4807485
- [23] T. Murotani, T. Shimanoe, S. Mitsui. *J. Crystal Growth*, **45**, 308 (1978); DOI: 10.1016/0022-0248(78)90453-0
- [24] E.C. Larkins, J.S. Harris. *Molecular Beam Epitaxy of High-Quality GaAs and AlGaAs*, ed. by Robin F.C. Farrow (William Andrew Inc., 1995)
- [25] F. Stietz, Th. Allinger, V. Polyakov, J. Woll, A. Goldmann, W. Erfurth, G.J. Lapeyre, J.A. Schaefer. *Appl. Surf. Sci.*, **104/105**, 169 (1996). DOI: 10.1016/S0169-4332(96)00140-7
- [26] M. Jalonen, M. Toivonen, P. Savolainen, J. Köngäs, M. Pessa. *Appl. Phys. Lett.*, **71** (4), 479 (1997). DOI: 10.1063/1.119584
- [27] J. Dekker, A. Tukiainen, N. Xiang, S. Orsila, M. Saarinen, M. Toivonen, M. Pessa, N. Tkachenko, H. Lemmetyinen. *J. Appl. Phys.*, **86** (7), 3709 (1999). DOI: 10.1063/1.371283
- [28] H.H. Yee, Ch.-P. Yu. *Appl. Opt.*, **42** (15), 2695 (2003). DOI: 10.1364/AO.42.002695
- [29] T. Bouragba, M. Mihailovic, F. Reveret, P. Disseix, J. Leymarie, A. Vasson, B. Damilano, M. Hugues, J. Massies, J.Y. Duboz. *J. Appl. Phys.*, **101** (7), 073510 (2007). DOI: 10.1063/1.2719289
- [30] H. Peyre, J. Camassel, W.P. Gillin, K.P. Homewood, R. Grey. *Mater. Sci. Eng. B*, **28** (1–3), 332 (1994). DOI: 10.1016/0921-5107(94)90077-9